# $K$-$L$ x-ray angular correlations in Cm, Pu, and Eu†

E. S. Macias and M. R. Zalutsky
*Department of Chemistry, Washington University, St. Louis, Missouri 63130*
(Received 5 October 1973; revised manuscript received 14 December 1973)

Angular correlations between $K$ and $L$ x rays in $^{245}$Cm, $^{239}$Pu, and $^{153}$Eu were measured. The x rays of Cm, Pu, and Eu were obtained from radioactive sources of 352-yr $^{249}$Cf, 32-yr $^{243}$Cm, and 242-day $^{153}$Gd, respectively. The $K$ x rays were detected with a cooled Ge(Li) spectrometer with energy resolution of 500-eV full width at half-maximum (FWHM) at 122 keV. The $L$ x rays were detected with a cooled Si(Li) spectrometer with energy resolution of 170 eV (FWHM) at 5.9 keV. Several corrections to the angular-correlation coefficients were made including a correction for the presence of silicon x-ray escape peaks. The corrected angular-correlation coefficients are:

| Cascade | $A_{22}$ (Cm) | $A_{22}$ (Pu) | $A_{22}$ (Eu) |
|---|---|---|---|
| $K\alpha_1$-$Ll$ | $(26.4 \pm 2.2) \times 10^{-2}$ | $(27.0 \pm 1.7) \times 10^{-2}$ | $(20.5 \pm 5.9) \times 10^{-2}$ |
| $K\alpha_1$-$L\alpha_{1+2}$ | $(4.48 \pm 0.58) \times 10^{-2}$ | $(4.74 \pm 0.40) \times 10^{-2}$ | $(2.73 \pm 0.39) \times 10^{-2}$ |
| $K\alpha_1$-$L\beta_{2+5+6+7+15}$ | $(5.14 \pm 0.80) \times 10^{-2}$ | $(3.09 \pm 0.57) \times 10^{-2}$ | $(5.7 \pm 2.0) \times 10^{-2}$ |

The results for the $K\alpha_1$-$L\alpha$ cascades are in good agreement with theoretical predictions. The results for the $K\alpha_1$-$L\beta$ cascade agree with theory for Eu but deviate significantly from theory for Pu and Cm. The results for the $K\alpha_1$-$Ll$ cascade in all three elements are lower than theoretical predictions. Results of similar studies of other elements are tabulated and compared to theory. For all elements studied the experimental angular-correlation coefficient agrees with the theoretical value for the $K\alpha_1$-$L\alpha$ cascade but is lower than the theoretical value for the $K\alpha_1$-$Ll$ cascade.

## I. INTRODUCTION

Recent measurements of the angular correlations of $K$-$L$ x-ray cascades have shown that predominantly electric dipole ($E1$) x-ray transitions have measurable amounts of magnetic quadrupole ($M2$) admixtures [1-7] However, the relationship between the extent of magnetic quadrupole admixtures in the x rays of a given element and the atomic number of that element requires more extensive experimental investigation. At present the angular correlations of the x rays of only a few elements have been measured and the analysis of many of these measurements has been hampered by difficulties caused by the inability to resolve the $K\alpha_1$ and $K\alpha_2$ x rays.

In this work the angular correlations between the $K\alpha_1$ and the several $L$ x-ray groups in Cm, Pu, and Eu were studied in three separate experiments. No experimental x-ray angular-correlation data were previously available for these elements. The use of high-resolution semiconductor spectrometers to detect the x rays of heavy elements such as Cm and Pu allowed complete resolution of the $K\alpha_1$ and $K\alpha_2$ x rays and removed the main source of experimental uncertainty present in many earlier experiments. Because the x-ray anisotropy increases with increasing atomic number, the angular-correlation coefficients measured in Pu and Cm were expected to be large. This should minimize experimental difficulties and in addition should give an accurate test of the theoretical predictions.

## II. EXPERIMENTAL PROCEDURES

The Pu x rays were obtained from a 100-$\mu$Ci source of 32-yr $^{243}$Cm which decays by $\alpha$ emission to several excited levels of $^{239}$Pu. These levels deexcite via $\gamma$ decay and internal conversion. The latter process leads to the emission of atomic x rays. Approximately 50% of the $\alpha$ decays of $^{243}$Cm are followed by the emission of $K$ x ray.[8] The $^{243}$Cm source was prepared by depositing a 1-mm-diam spot of $^{243}$Cm$(NO_3)_3$ on a 0.5-mm-thick aluminum disk covered by 2.5-mm berylium.

The Eu x rays were emitted from a 50-$\mu$Ci source of 242-day $^{153}$Gd which decays by electron capture to excited states of $^{153}$Eu. The excited $^{153}$Eu levels undergo $K$ and $L$ internal conversion. Decay by both electron capture and internal conversion leads to the emission of Eu x rays. The $^{153}$Gd source was prepared by depositing $^{153}GdCl_3$ on $6 \times 10^{-3}$-mm-thick Mylar film.

Ten $\mu$Ci of 352-yr $^{249}$Cf served as the source of Cm x rays. The source was 1 mm in diameter deposited on a 0.15-mm aluminum disk covered with 0.25 mm of berylium. The x rays are emitted

following the internal conversion of $^{245}$Cm nuclear levels populated in the $\alpha$ decay of $^{249}$Cf.

During the measurements a source was placed in the center of an angular-correlation table where it was viewed by both the $K$ and $L$ x-ray detectors. The $K$ x rays were detected in a 10-mm planar Ge(Li) crystal with a sensitive depth of 5 mm. The crystal housing was fitted with a 0.12-mm-thick berylium window. This detector, which had energy resolution of 500-eV full width at half-maximum (FWHM) at 122 keV, was able to completely resolve the $K\alpha_1$ and $K\alpha_2$ x rays of Pu and Cm. However these same x rays in Eu were only partially resolved as shown in Fig. 1.

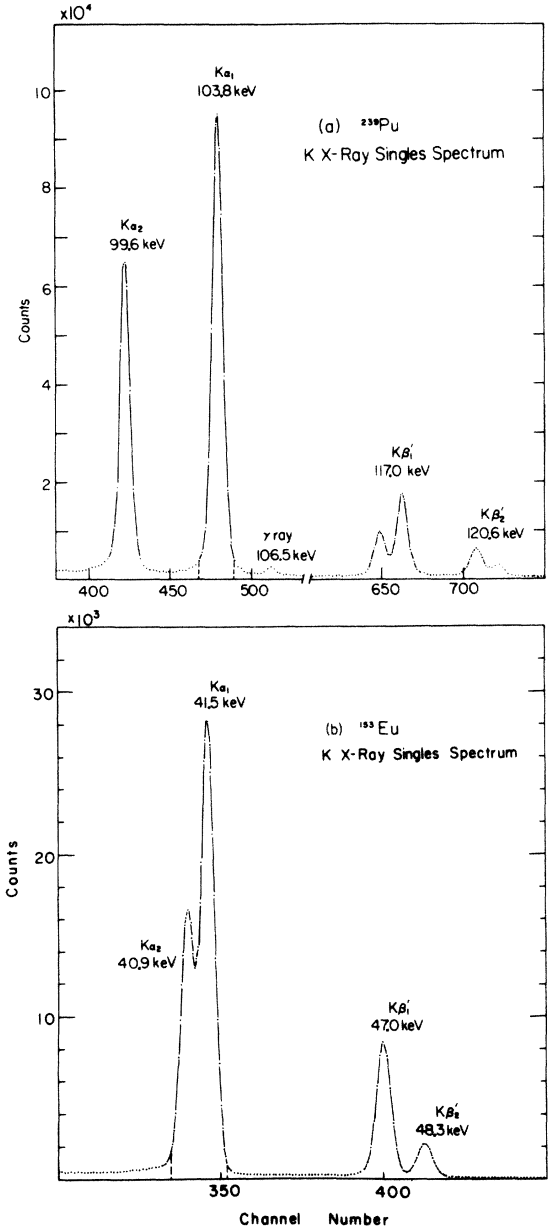


FIG. 1. (a) Spectrum of Pu $K$ x rays detected in the Ge(Li) detector. The broken line indicates the position of the $K\alpha_1$ gate used. (b) Spectrum of Eu $K$ x rays detected in the Ge(Li) detector. The broken line indicates the position of the $K\alpha_{1+2}$ gate used.

The $L$ x rays were detected in a 4-mm-diam planar Si(Li) crystal with a sensitive depth of 3 mm. The crystal housing was fitted with a 0.05-mm-thick berylium window. The energy resolution of the Si(Li) detector was 170 eV (FWHM) at 5.9 keV. The detectors were capable of being moved on the circumference of the angular-correlation goniometer and were kept at a constant distance from the source. Each detector was shielded laterally by a tapered collimator consisting of a lead core sandwiched between layers of brass and aluminum. These collimators minimized the contribution of erroneous coincidences due to scattering of radiation from one detector to the other.

X-ray coincidence spectra were obtained with a standard fast-slow coincidence system employing cross-over timing with a resolving time $2\tau$ of 60 nsec. A schematic diagram of the electronic system is shown in Fig. 2. Pulses from the low-noise preamplifiers connected to each detector were sent to individual amplifiers with shaping time constants of 0.5 $\mu$sec for optimum timing characteristics. The bipolar output of each amplifier was sent to timing single-channel analyzers (SCA) which were set to pass the $K\alpha_1$ x ray of Pu or Cm or the unresolved $K\alpha_1$ and $K\alpha_2$ x rays of Eu detected in the Ge(Li) crystal and $L$ x rays detected in the Si(Li) crystal. The preamplified signals from the Si(Li) x-ray detector were sent to an additional amplifier with a shaping time constant of 6 $\mu$sec for optimum energy resolution. The $L$ x-ray coincidence spectrum was stored in a 1024-channel pulse-height analyser. Typical Pu and Eu $L$ x-ray singles spectra detected in the Si(Li) x-ray spectrometer are shown in Fig. 3. As a monitor of the experimental system the number of output pulses from each SCA and from the fast coincidence module were stored in separate scalers.

The $L$ x-ray spectrum in coincidence with $K\alpha_1$ x rays of Pu and Cm were measured at nine and five different angles between the two detectors, respectively. The angles between the directions of the radiations striking the two detectors were 90°, 110°, 140°, 160°, 180°, and their equivalent angles in the 180–270° quadrant for Pu. Coincidence spectra were measured from 90° to 270° in steps of 45° for Cm. The spectrum at each angle was accumulated for 10 000 sec. A single data set for Pu consisted of one measurement

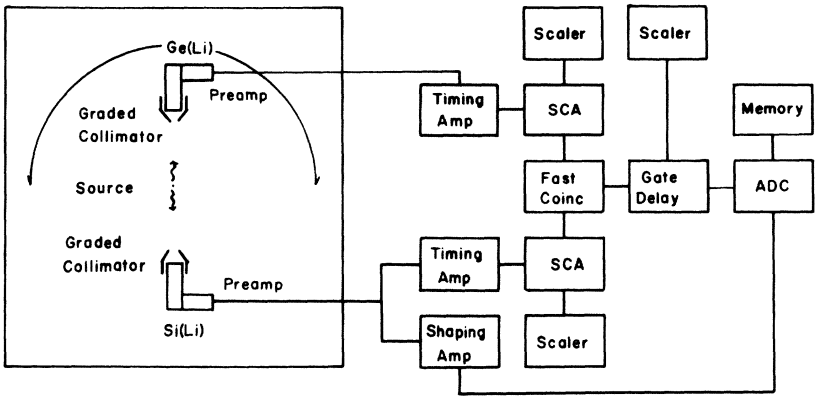


FIG. 2. Schematic diagram of the electronic system.

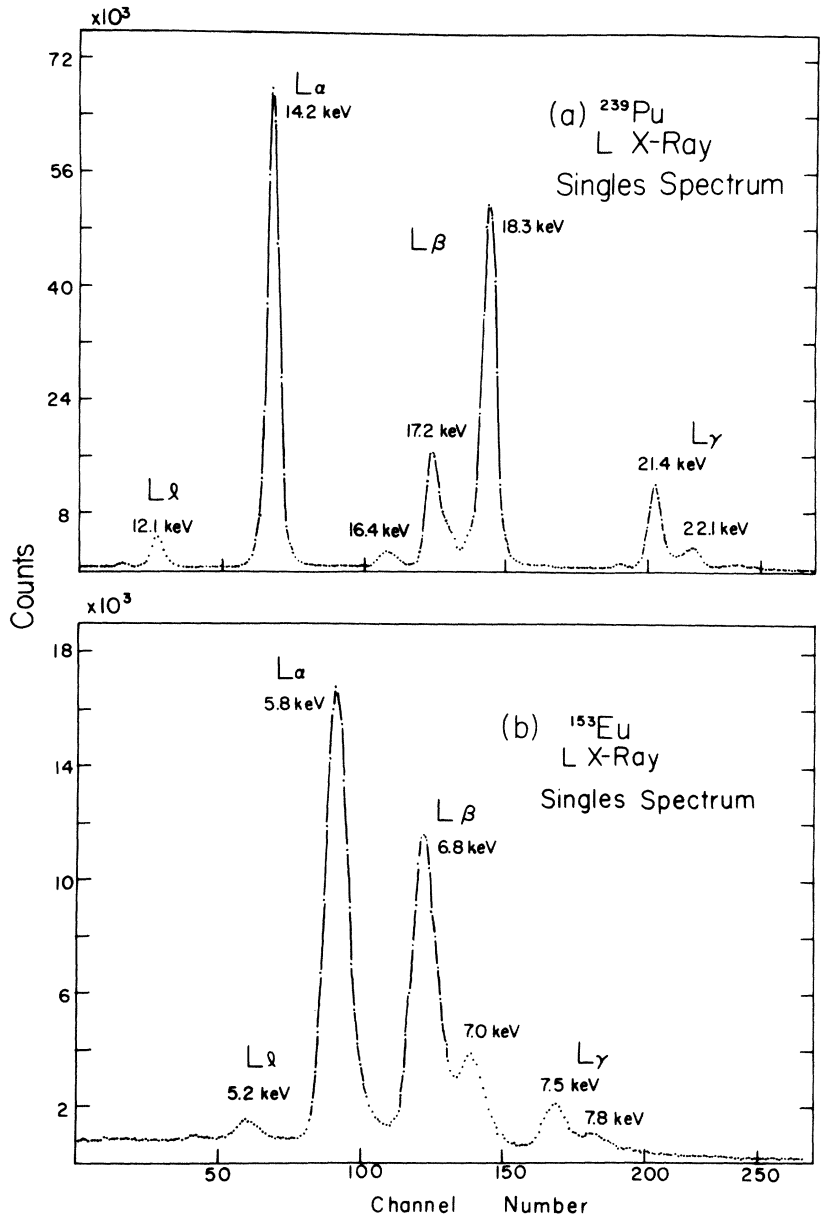


FIG. 3. (a) Spectra of Pu $L$ x rays detected in the Si(Li) detector. (b) Spectra of Eu $L$ x rays detected in the Si(Li) detector.

at each of the nine angles and a second measurement at 180°. A single data set for Cm consisted of a 24-hr measurement at each of the five angles and a second measurement at 180°. The angles were selected randomly in order to minimize error caused by electronic instabilities. Angles symmetric about 180° were added together for data analysis. The Eu x-ray spectrum in coincidence with $K\alpha_1$ and $K\alpha_2$ x rays was recorded as described above for Pu except that only seven angles of measurements were made from 90° to 270° in steps of 30°. A total of 10, 13, and 15 data sets were accumulated for the experiments on Cm, Pu, and Eu, respectively. The coincidence data at each angle were normalized to the numbers of $K\alpha_1$ x rays in the Pu and Cm experiments and $K\alpha_1$ plus $K\alpha_2$ x rays in the Eu experiment detected in the Ge(Li) spectrometer. This normalization procedure removed the effects of source decentering (< 0.5%) and radioactive decay. Background, determined in regions of the spectrum where there were no x-ray peaks, was subtracted from each peak. The contribution from random coincidences was determined by taking long measurements with an additional 640-nsec relative delay between the output of the two detectors. The data were corrected for these random coincidences which were found to be angle independent. In the Pu and Cm x-ray experiments, the extent of scattering of x rays or $\gamma$ rays between detectors was determined by placing a 0.50-mm copper absorber on the face of the radioactive source toward the $L$ x-ray detector. In the Eu x-ray experiment this effect was determined by placing a 0.50-mm aluminum absorber on the face of the $^{153}$Gd source toward the $L$ x-ray detector. Contributions due to scattering were found to be negligible at all angles for $^{243}$Cm and $^{249}$Cf. In $^{153}$Gd it was found that scattering between detectors was negligible at all angles except 180° and the data were corrected accordingly. The number of coincidence events due to a Compton-scattered $K$ x ray in one detector and a Compton-scattered $\gamma$ ray in the other detector were subtracted from the $^{153}$Gd scattering measurements. The magnitude of this effect, which is corrected for in the normal angular-correlation data by background subtraction, was determined by taking a second set of scattering coincidence data with a 0.7-cm-thick lead shield between the two detectors.

## III. DATA ANALYSIS

After normalization and subtraction of background and random coincidence events, the data for all cascades were fitted by a weighted least-squares procedure to an expression of the form $N(\theta) = a_0 + a_2 P_2(\cos\theta)$, where $N(\theta)$ is the corrected number of counts accumulated at the angle $\theta$ and $P_2(\cos\theta)$ is the second-order Legendre polynomial. The resultant expansion coefficients were normalized yielding an angular-correlation function of the form

$$W(\theta) = 1 + A_{22} P_2(\cos\theta) , \tag{1}$$

where $A_{22} = a_2/a_0$. Because the spin of the intermediate atomic state in the x-ray cascade is $\frac{3}{2}$ the coefficients of all higher-order terms in the Legendre-polynomial expansion must be zero.[9] However as an additional check on the experiment the data for all cascades were also fit to expressions with a third term, $a_4 P_4(\cos\theta)$, where $P_4(\cos\theta)$ is the fourth-order Legendre polynomial, and in all cases $a_4$ was found to be zero within experimental error. The finite solid angle subtended by each detector was determined by extrapolating the data of Camp and Van Lehn[10] and both were found to be negligible.

Because the $K\alpha_1$ and $K\alpha_2$ x rays of Eu were unresolved in the Ge(Li) detector, the experimental angular-correlation coefficients were corrected for the presence of isotropic coincidence events between $K\alpha_2$ and $L$ x rays.[11] This correction factor, $F_{K\alpha_2}(X)$, for the cascade $K\alpha$-$X$ is given as follows:

$$F_{K\alpha_2}(X) = \frac{\text{all contributions to cascade } K\alpha\text{-}X}{\text{anisotropic contributions to cascade } K\alpha\text{-}X} . \tag{2}$$

The data for the $K\alpha$-$L\alpha$ cascade in Eu consist of three types of events: (i) anisotropic coincidences between $K\alpha_1$ and $L\alpha_1$ or $L\alpha_2$ x rays; (ii) isotropic coincidences between $K\alpha_2$ and $L\eta$ x rays (in Eu the $L\alpha$ and $L\eta$ x rays are unresolved)[12]; (iii) isotropic coincidence events due to a three-step cascade of a $K\alpha_2$ x ray followed by an $L_2$-$L_3X$ Coster-Kronig radiationless transition and then an $L\alpha_1$ or $L\alpha_2$ x ray. The magnitude of each contribution is calculated using the following expressions:

$$\text{Contribution (i) } (K\alpha_1)\omega_3[\Gamma(L\alpha_1) + \Gamma(L\alpha_2)]/\Gamma_{L3} , \tag{3}$$

$$\text{Contribution (ii) } (K\alpha_2)\omega_2\Gamma(L\eta)/\Gamma_{L2} , \tag{4}$$

$$\text{Contribution (iii) } (K\alpha_2) f_{23}\omega_3[\Gamma(L\alpha_1) + \Gamma(L\alpha_2)]/\Gamma_{L3} , \tag{5}$$

where $\Gamma(X)$ is the radiative transition width for transition $X$, $\Gamma_{Li}$ is the total radiative width of the $L_i$ subshell, $\omega_i$ is the fluorescence yield of the $L_i$ subshell, and $f_{23}$ if the $L_2$-$L_3X$ Coster-Kronig transition probability. In Eu $\omega_2 \simeq \omega_3$[13] therefore $F_{K\alpha_2}(L\alpha)$ is expressed as follows:

$$F_{K\alpha_2}(L\alpha) = 1 + \frac{\Gamma(K\alpha_2)}{\Gamma(K\alpha_1)} \left( \frac{\Gamma_{L3}\Gamma(L\eta)}{\Gamma_{L2}[\Gamma(L\alpha_1) + \Gamma(L\alpha_2)]} + f_{23} \right). \quad (6)$$

The $K\alpha$-$Ll$ cascade consists of two components: (i) anisotropic $K\alpha_1$-$Ll$ coincidences whose contribution is given by

$$(K\alpha_1)\omega_3\Gamma(Ll)/\Gamma_{L3} \quad (7)$$

and (ii) isotropic $K\alpha_2$-$(L_2$-$L_3X)$-$Ll$ coincidences whose contribution is given by

$$\Gamma(K\alpha_2)f_{23}\omega_3\Gamma(Ll)/\Gamma_{L3} \, . \quad (8)$$

Therefore the correction factor to the $K\alpha_1$-$Ll$ cascade due to the $K\alpha_2$ x rays in the $K$ x-ray gate is

$$F_{K\alpha_2}(Ll) = 1 + \frac{\Gamma(K\alpha_2)}{\Gamma(K\alpha_1)} f_{23} \, . \quad (9)$$

The $K\alpha$-$L\beta$ cascade consists of the following contributions: (i) anisotropic $K\alpha_1$-$(L\beta_2, L\beta_5, L\beta_6, L\beta_7,$ or $L\beta_{15})$ coincidence events whose contribution is given by

$$(K\alpha_1)\omega_3[\Gamma(L\alpha_2) + \Gamma(L\beta_5) + \Gamma(L\beta_6) + \Gamma(L\beta_7) + \Gamma(L\beta_{15})]/\Gamma_{L3}\,; \quad (10)$$

(ii) isotropic contributions due to $K\alpha_2$-$(L\beta_1$ or $L\beta_{17})$ coincidence events whose contribution is given by

$$(K\alpha_2)\omega_2[\Gamma(L\beta_1) + \Gamma(L\beta_{17})]/\Gamma_{L2}\,; \quad (11)$$

and (iii) isotropic contributions due to $K\alpha_2$-$(L_2$-$L_3X)$-$(L\beta_2, L\beta_5, L\beta_6, L\beta_7,$ or $L\beta_{15})$ coincidence events whose contribution is given by

$$(K\beta_2)f_{23}\omega_3[\Gamma(L\beta_2) + \Gamma(L\beta_5) + \Gamma(L\beta_6) + \Gamma(L\beta_7) + \Gamma(L\beta_{15})]/\Gamma_{L3} \, . \quad (12)$$

The correction factor $F_{K\alpha_2}$ is given by

$$F_{K\alpha_2}(L\beta) = 1 + \frac{\Gamma(K\alpha_2)}{\Gamma(K\alpha_1)} \left( \frac{\Gamma_{L3}[\Gamma(L\beta_1) + \Gamma(L\beta_{17})]}{\Gamma_{L2}[\Gamma(L\beta_2) + \Gamma(L\beta_5) + \Gamma(L\beta_6) + \Gamma(L\beta_7) + \Gamma(L\beta_{15})]} + f_{23} \right) . \quad (13)$$

The $F_{K\alpha_2}$ factors, evaluated using the theoretical radiative transition rates calculated by Scofield[12] are given in Table I. The $f_{23}$ value used for Eu is $f_{23} = 0.172 \pm 0.015$ which was determined by Zalutsky and Macias[14] using the $K$-$L$ x-ray coincidence method.

A second correction to the $A_{22}$ coefficients was made for unwanted coincidence events due to a $K$ and $L$ x ray each resulting from the migration of an electron hole formed in a different nuclear decay process in the same atom within a time shorter than the resolving time of the coincidence circuit. In the decay of $^{243}$Cm these nuclear cascade events result from two successive internal

TABLE I. X-ray angular-correlation results for Cm, Pu, and Eu.

| | Cascade | $A_{22}$ (experimental) [a] | $F_{K\alpha_2}$ [b] | $F_{\text{cascade}}$ [c] | $F_{\text{escape}}$ [d] | $A_{22}$ (corrected) |
|---|---|---|---|---|---|---|
| $^{245}$Cm | $K\alpha_1$-$Ll$ | $(20.6 \pm 1.7) \times 10^{-2}$ | ··· | $1.254 \pm 0.017$ | $1.023 \pm 0.003$ | $(26.4 \pm 2.2) \times 10^{-2}$ |
| | $K\alpha_1$-$L\alpha$ | $(3.57 \pm 0.42) \times 10^{-2}$ | ··· | $1.254 \pm 0.017$ | ··· | $(4.48 \pm 0.58) \times 10^{-2}$ |
| | $K\alpha_1$-$L\beta$ | $(4.10 \pm 0.60) \times 10^{-2}$ | ··· | $1.254 \pm 0.017$ | ··· | $(5.14 \pm 0.80) \times 10^{-2}$ |
| $^{239}$Pu | $K\alpha_1$-$Ll$ | $(20.4 \pm 1.3) \times 10^{-2}$ | ··· | $1.289 \pm 0.013$ | $1.026 \pm 0.004$ | $(27.0 \pm 2.2) \times 10^{-2}$ |
| | $K\alpha_1$-$L\alpha$ | $(3.36 \pm 0.31) \times 10^{-2}$ | ··· | $1.289 \pm 0.013$ | ··· | $(4.74 \pm 0.40) \times 10^{-2}$ |
| | $K\alpha_1$-$L\beta$ | $(2.40 \pm 0.44) \times 10^{-2}$ | ··· | $1.289 \pm 0.013$ | ··· | $(3.09 \pm 0.57) \times 10^{-2}$ |
| $^{153}$Eu | $K\alpha_1$-$Ll$ | $(13.8 \pm 4.0) \times 10^{-2}$ | $1.095 \pm 0.008$ | $1.314 \pm 0.007$ | $1.025 \pm 0.004$ | $(20.5 \pm 6.0) \times 10^{-2}$ |
| | $K\alpha_1$-$L\alpha$ | $(1.87 \pm 0.27) \times 10^{-2}$ | $1.111 \pm 0.008$ | $1.314 \pm 0.007$ | ··· | $(2.73 \pm 0.39) \times 10^{-2}$ |
| | $K\alpha_1$-$L\beta$ | $(1.04 \pm 0.35) \times 10^{-2}$ | $4.2 \pm 0.3$ | $1.314 \pm 0.007$ | ··· | $(5.6 \pm 1.9) \times 10^{-2}$ |

[a] These values are the result of a weighted least-squares fit to the data which have been corrected for random coincidences.

[b] Correction for the presence of isotropic $K\alpha_2$-$L$ coincidence events [see Eq. (1) in the text].

[c] Correction for the effect of nuclear cascade events as described in Sec. III in the text.

[d] Correction for the presence of a Si x-ray escape peak in the main $L$ x-ray peak.

conversion processes in the $^{239}$Pu nucleus. In $^{153}$Gd decay these events occur whenever electron capture is followed by the internal conversion of a $^{153}$Eu level as well as when two successive internal conversion decays occur in the $^{153}$Eu nucleus. The magnitude of this nuclear-cascade effect was determined by measuring the $L$ x-ray spectrum in coincidence with $K\beta$ x rays. A $K\beta$ x ray results from a transition between the $K$ shell and the $M$ or $N$ shell, while an $L$ x ray results from a transition from the $L$ shell. Therefore an $L$ x ray can be in coincidence with $K\beta$ x ray only when each x ray originates from the migration of a hole formed in different decay processes in the same nucleus or from random coincidence events. Nuclear events amounted to (20.3 ± 1.0)%, (22.4 ± 0.8)%, and (23.9 ± 0.4)% of the total coincidence events in $^{249}$Cf, $^{243}$Cm, and $^{153}$Gd decay, respectively.

A final correction to the angular-correlation coefficient was made for the presence of a silicon x-ray escape peak under an x-ray photopeak. This will occur when

$$\Delta E_x = 1.74 \pm \text{FWTM keV},$$

where $\Delta E_x$ is the energy difference between two x rays and FWTM is the full width at tenth maximum of the Si(Li) detector at $E_x$. In the present experiments the Si(Li) detector had a FWTM of < 500 eV at 14.4 keV. The x-ray escape peak will cause a measurable change in the angular correlation only if the higher-energy x ray is much more intense than the lower-energy x ray. The $K\alpha_1$-$Ll$ angular correlation must be corrected for the presence of the x-ray escape peak from the $L\alpha_{1+2}$ x rays in $^{239}$Pu and $^{243}$Cm, and the $L\beta_2$ x ray in $^{153}$Eu. This correction was not necessary for the other $K$-$L$ x ray cascades. Using the absolute photon and x-ray escape-peak efficiences for the Si(Li) detector employed in this work,[15] it was determined that a contribution of (2.6 ± 0.3)%, (3.2 ± 0.3)%, and (2.5 ± 0.3)% of the total $Ll$ peak in $^{245}$Cm, $^{239}$Pu, and $^{153}$Eu, respectively, is due to a silicon x-ray escape peak.

## IV. RESULTS AND DISCUSSION

The values of the angular-correlation coefficients corrected for Coster-Kronig transitions, cascade effects, and x-ray escape peaks are given for Cm, Pu, and Eu in Table I. The data and fitted curves are shown in Fig. 4. Although the Si(Li) detector resolved the $L\beta$ x rays of Cm and Pu into several subgroups, these x rays were analyzed as a single $L\beta$ x-ray group to facilitate comparison with measurements in other elements. The $K\alpha$-$L\gamma$ x-ray

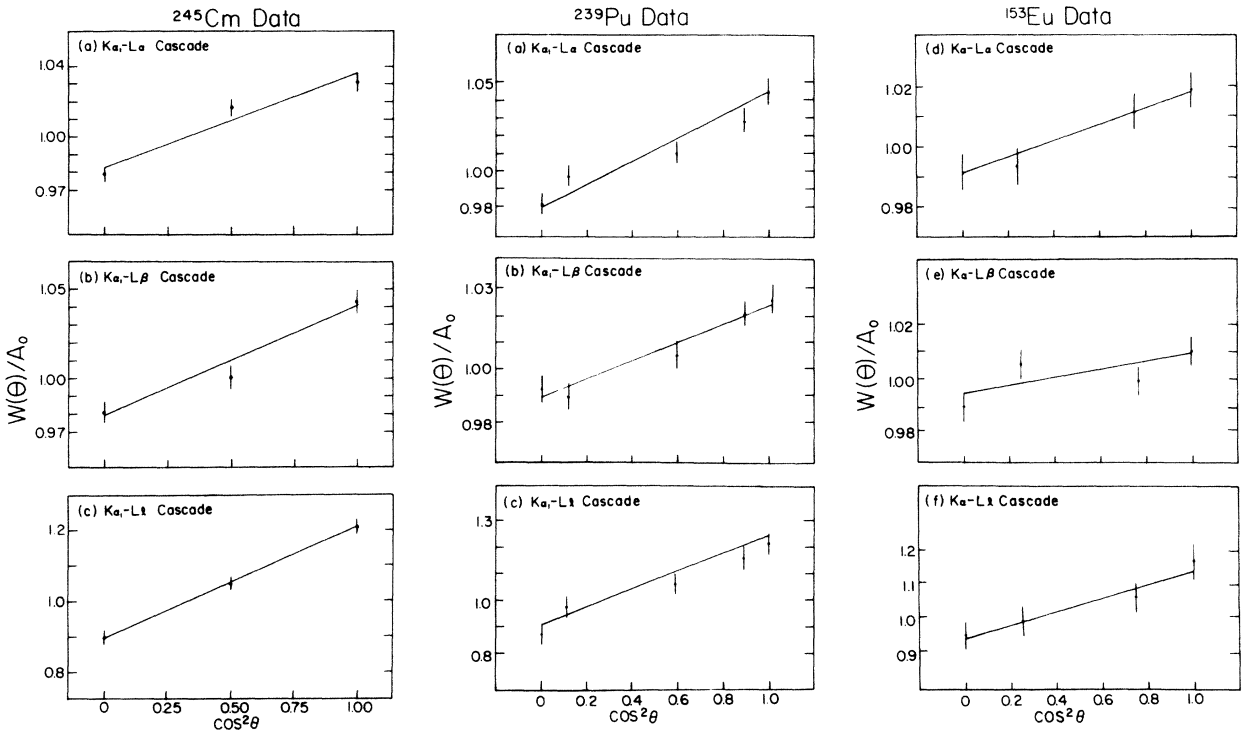


FIG. 4. Results of the angular-correlation measurements of $K$-$L$ x-ray cascades in $^{245}$Cm, $^{239}$Pu, and $^{153}$Eu. The solid line is a least-squares fit of the data to an equation of the form $N(\theta) = a_0 + a_2 P_2(\cos\theta)$.

angular correlation was also measured as a check on the experimental system. Coincidence events for this cascade can only occur when a $K\alpha_2$-$L\gamma$ cascade occurs or when a nuclear cascade leads to a $K\alpha_1$ x ray for one nuclear decay followed by a $L\gamma$ x ray from another nuclear decay in the same atom. Both types of events have an isotropic angular distribution. The angular-correlation coefficients measured for the $K\alpha_1$-$L\gamma$ cascade in $^{245}$Cm and $^{239}$Pu were both $A_{22} = (1 \pm 2) \times 10^{-2}$ and for the $K\alpha_{1+2}$-$L\gamma$ cascade in $^{153}$Eu was $A_{22} = (-0.9 \pm 1.4) \times 10^{-2}$.

The experimental results for the x-ray angular correlation of the $K\alpha_1$-$L\alpha_{1+2}$ cascade in Cm, Pu, and Eu are in good agreement with Scofield's theoretical predictions[12] for this cascade, although the $^{239}$Pu result is slightly higher than the prediction. A summary of all data for this cascade in all elements measured is given in Table II and Fig. 5. The data for Tl, Tb, and Nd as well as Eu have been corrected for the presence of $K\alpha_2$ x rays in the $K$ x-ray gate which leads to isotropic coincidence events with x rays from the $L_3$ level as explained in Sec. III. The correction factors $F_{K\alpha_2}(L\alpha)$ given in Table II were calculated using Eq. (6). The data show good agreement with the theoretical predictions which include electric dipole–magnetic-quadrupole ($E1/M2$) mixing (the dotted line in Fig. 5). The solid line in that figure is the expected value for pure $E1$ transitions. It is clear that the latter assumption leads to poor agreement with experimental results. The results of the measurements of $^{245}$Cm x rays reported here indicate that the high value for this cascade in $^{239}$Pu is not a general trend at very high atomic numbers.

TABLE II. Measured and theoretical $K$-$L$ x-ray angular-correlation coefficients.

| Cascade | $Z$ | Isotope | $A_{22}$ (experimental) [a] | $F_{K\alpha_2}$ [b] | $A_{22}$ (corrected) | Theoretical [c] prediction | Reference |
|---|---|---|---|---|---|---|---|
| $K\alpha_1$-$L\alpha$ | 60 | $^{145}$Nd | $(2.7 \pm 0.3) \times 10^{-2}$ | 1.09 ± 0.11 [e] | $(2.9 \pm 0.4) \times 10^{-2}$ | 0.0302 | Ref. 5 |
| | 63 | $^{153}$Eu [d] | $(2.46 \pm 0.36) \times 10^{-2}$ | 1.111 ± 0.008 [f] | $(2.73 \pm 0.39) \times 10^{-2}$ | 0.0309 | This work |
| | 65 | $^{159}$Tb | $(2.6 \pm 0.5) \times 10^{-2}$ | 1.084 ± 0.007 [g] | $(2.8 \pm 0.5) \times 10^{-2}$ | 0.0313 | Ref. 5 |
| | 73 | $^{181}$Ta [d] | $(2.97 \pm 0.33) \times 10^{-2}$ | ··· | $(2.97 \pm 0.33) \times 10^{-2}$ | 0.0333 | Ref. 6 |
| | 81 | $^{203}$Tl | $(3.63 \pm 0.32) \times 10^{-2}$ | 1.095 ± 0.006 [h] | $(3.97 \pm 0.35) \times 10^{-2}$ | 0.0358 | Ref. 3 |
| | 82 | $^{207}$Pb | $(3.63 \pm 0.20) \times 10^{-2}$ | ··· | $(3.63 \pm 0.20) \times 10^{-2}$ | 0.0361 | Ref. 7 |
| | 92 | $^{233}$U | $(4.12 \pm 0.57) \times 10^{-2}$ | ··· | $(4.12 \pm 0.57) \times 10^{-2}$ | 0.0398 | Ref. 2 |
| | 94 | $^{239}$Pu [d] | $(4.74 \pm 0.40) \times 10^{-2}$ | ··· | $(4.74 \pm 0.40) \times 10^{-2}$ | 0.0406 | This work |
| | 96 | $^{245}$Cm [d] | $(4.48 \pm 0.58) \times 10^{-2}$ | ··· | $(4.48 \pm 0.58) \times 10^{-2}$ | 0.0415 | This work |
| $K\alpha_1$-$L\beta$ | 60 | $^{145}$Nd | $(0.5 \pm 0.4) \times 10^{-2}$ | 4.3 ± 0.3 [e] | $(2.1 \pm 1.7) \times 10^{-2}$ | 0.0459 | Ref. 5 |
| | 63 | $^{153}$Eu [d] | $(1.37 \pm 0.46) \times 10^{-2}$ | 4.2 ± 0.3 [f] | $(5.7 \pm 2.0) \times 10^{-2}$ | 0.0470 | This work |
| | 65 | $^{159}$Tb | $(-0.1 \pm 0.5) \times 10^{-2}$ | 4.2 ± 0.3 [g] | $(-0.4 \pm 2.1) \times 10^{-2}$ | 0.0478 | Ref. 5 |
| | 73 | $^{181}$Ta [d] | $(3.44 \pm 0.94) \times 10^{-2}$ | ··· | $(3.44 \pm 0.94) \times 10^{-2}$ | 0.0516 | Ref. 6 |
| | 81 | $^{203}$Tl | $(1.31 \pm 0.36) \times 10^{-2}$ | 3.8 ± 0.3 [h] | $(5.0 \pm 1.4) \times 10^{-2}$ | 0.0552 | Ref. 3 |
| | 82 | $^{207}$Pb | $(5.6 \pm 0.8) \times 10^{-2}$ | ··· | $(5.6 \pm 0.8) \times 10^{-2}$ | 0.0558 | Ref. 7 |
| | 94 | $^{239}$Pu [d] | $(3.09 \pm 0.57) \times 10^{-2}$ | ··· | $(3.09 \pm 0.57) \times 10^{-2}$ | 0.0653 | This work |
| | 96 | $^{245}$Cm [d] | $(5.14 \pm 0.80) \times 10^{-2}$ | ··· | $(5.14 \pm 0.80) \times 10^{-2}$ | 0.0661 | This work |
| $K\alpha_1$-$Ll$ | 60 | $^{145}$Nd | 0.15 ± 0.03 | 1.08 ± 0.11 [e] | 0.16 ± 0.04 | 0.273 | Ref. 5 |
| | 63 | $^{153}$Eu [d] | 0.186 ± 0.054 | 1.095 ± 0.008 [f] | 0.204 ± 0.059 | 0.275 | This work |
| | 65 | $^{159}$Tb | 0.14 ± 0.05 | 1.069 ± 0.007 [g] | 0.15 ± 0.05 | 0.277 | Ref. 5 |
| | 73 | $^{181}$Ta [d] | 0.204 ± 0.019 | ··· | 0.204 ± 0.019 | 0.284 | Ref. 6 |
| | 81 | $^{203}$Tl | 0.218 ± 0.020 | 1.095 ± 0.007 [h] | 0.239 ± 0.022 | 0.293 | Ref. 3 |
| | 82 | $^{207}$Pb | 0.277 ± 0.017 | ··· | 0.277 ± 0.017 | 0.294 | Ref. 7 |
| | 94 | $^{239}$Pu [d] | 0.270 ± 0.017 | ··· | 0.270 ± 0.017 | 0.309 | This work |
| | 96 | $^{245}$Cm [d] | 0.264 ± 0.022 | ··· | 0.264 ± 0.022 | 0.311 | This work |

[a] These values have been corrected for the effect of random coincidences, nuclear cascades, scattering, and the finite solid angle subtended by the detectors.

[b] Correction for the presence of isotropic $K\alpha_2$-$L$ coincidence events [see Eq. (1) in the text]. No correction is needed for Ta, Pb, U, Pu, or Cm data because the $K\alpha_2$ x-ray does not appear in the $K\alpha$ gate.

[c] Reference 12.

[d] $A_{22}$ values for this element have been corrected for the effect of silicon x-ray escape peaks.

[e] Calculated using $f_{23} = 0.142 \pm 0.014$ from M. H. Chen, B. Craseman, and V. O. Kostroun, Phys. Rev. A 4, 1 (1971); E. J. McGuire, Phys. Rev. A 3, 587 (1971). We have assigned a 10% uncertainty to this theoretical value.

[f] Calculated using $f_{23} = 0.172 \pm 0.015$ from Ref. 14.

[g] Calculated using $f_{23} = 0.124 \pm 0.012$ from P. V. Rao (private communication, 1973).

[h] Calculated using $f_{23} = 0.16 \pm 0.01$ from S. Mohan, thesis (Georgia Institute of Technology, 1972) (unpublished).

The $A_{22}$ value for the $K\alpha_1$-$L\beta$ cascade in Eu agrees with the theoretical prediction, however the results for this cascade in Cm and Pu are much lower than theory. The existing data for this cascade, summarized in Table II and Fig. 5(b), show no obvious trend. The agreement with theoretical predictions is not particularly good but this is not too surprising in light of the fact that the $L\beta$ x ray consists of several transitions. A slight change in the calculated intensity for each transition could change the theoretical prediction greatly. This is particularly true for the results in the lighter elements where the $K\alpha_1$ and $K\alpha_2$ x rays are not resolved. In this case the isotropic $K\alpha_2$-$L\beta_1$ cascade accounts approximately 86% of the total coincidence intensity which adds to the experimental difficulties and makes the correction factor $F_{K\alpha_2}(L\beta)$ very large.

The $K\alpha_1$-$Ll$ cascade is of particular interest because it is composed of a single $L$ x ray and thus the interpretation of this cascade does not depend on calculated $L$ x-ray intensities. In addition the $A_{22}$ value for the $K\alpha_1$-$Ll$ cascade is 5–10 times larger than the $A_{22}$ value for the $K$-$L\alpha_{1+2}$ x-ray cascades. Unfortunately, this is offset by the $Ll$ intensity which is a factor of 12–25 times less intense than the $L\alpha_1$ transition.[12]

The results for the $K\alpha_1$-$Ll$ cascade in curium, plutonium, and europium are all lower than the theoretical predictions. The existing data for this cascade are summarized in Table II and Fig. 5(c). The data show a general trend of increasing angular-correlation coefficient $A_{22}$ with increasing atomic number as predicted by Scofield's calculations. However the data in every case are lower than the theoretically predicted results which assume $M2$ admixtures. This trend cannot be reproduced if the x rays are assumed to be pure electric dipole transitions. In lighter elements, where the energy difference between the $L\alpha$ and the $Ll$ transitions is small, the low $A_{22}$ value may be at least partially explained if the highly anisotropic $Ll$ peak is not fully resolved from the nearly isotropic $L\alpha$ x ray. In the case of curium and plutonium, where these x rays are very well resolved, this effect does not explain the discrepancy with the predicted results.

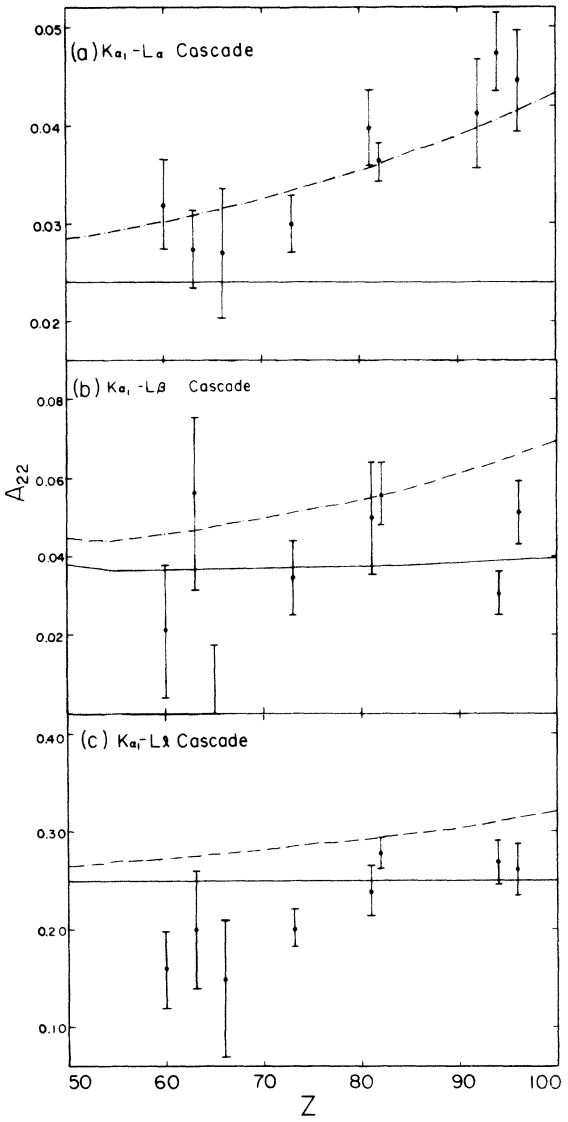


FIG. 5. Values of the normalized angular-correlation coefficient $A_{22}$ calculated from theory as a function of atomic number for (a) $K\alpha_1$-$L\alpha_{1+2}$, (b) $K\alpha_1$-$L\beta$, (c) $K\alpha_1$-$Ll$ cascades. The upper dashed curve in each frame was calculated assuming the x-ray transitions $E1/M2$ admixtures (from Ref. 12). The lower solid curve in each frame was calculated assuming the x rays were pure $E1$ transitions. The experimental values from this work and Refs. 2, 3, and 5–7 are also shown.

## ACKNOWLEDGMENTS

We wish to thank Dr. E. K. Hulet of Lawrence Livermore Laboratory for providing us with the $^{243}$Cm and $^{249}$Cf sources. We would also like to acknowledge a special debt to Gilbert Krechman and Paul Shockley for the skillful construction of the angular-correlation table and collimators.

## APPENDIX

The characteristic x rays referred to in this paper are identified below according to the nomenclature of Bearden.[16]

(i) *K series.*

$K\alpha_1$ $KL_3$ ,

$K\alpha_2$ $KL_2$ ,

$K\beta$ $\begin{cases} KM_{2,3,4,5}, \\ KN_{2,3,4,5}. \end{cases}$

(ii) *L series.*

$Ll$ $L_3M_1$ ,

$L\alpha_1$ $L_3M_5$ ,

$L\alpha_2$ $L_3M_4$ ,

$L\beta_1$ $L_2M_4$ ,

$L\beta_2$ $L_3M_5$ ,

$L\beta_5$ $L_3O_{4,5}$ ,

$L\beta_6$ $L_3N_1$ ,

$L\beta_7$ $L_3O_1$ ,

$L\beta_{15}$ $L_3N_4$ ,

$L\gamma$ $\begin{cases} L_1N_{2,3}, \\ L_1O_{2,3}, \\ L_2N_{1,4,5}, \\ L_2O_{1,4}, \end{cases}$

$L\eta$ $L_2M_1$ .

---

*Work supported in part by The Research Corporation.

[1]E. S. Macias and M. R. Zalutsky, in *Proceedings of the International Conference on Inner Shell Ionization Phenomena and Future Applications*, edited by R. W. Fink, S. T. Manson, J. M. Palms, and P. Venugopala Rao, U.S.A.E.C. Report No. CONF-720404 (U.S. GPO, Washington, D.C., 1973), p. 267.

[2]A. L. Catz and L. Finkel, in Ref. 1, p. 257.

[3]A. L. Catz and E. S. Macias, Phys. Rev. A 3, 849 (1971).

[4]A. L. Catz, Phys. Rev. Lett. 24, 137 (1970); A. L. Catz, Phys. Rev. A 2, 634 (1970).

[5]A. L. Catz and E. S. Macias, Phys. Rev. A (to be published).

[6]M. R. Zalutsky, E. S. Macias, and A. L. Catz, Phys. Rev. A (to be published).

[7]A. L. Catz and H. N. Erten (unpublished).

[8]Y. A. Ellis and A. H. Wapstra, Nucl. Data B 3, 2 (1969).

[9]H. Frauenfelder and R. M. Steffen, in *Alpha-, Beta- and Gamma-Ray Spectroscopy*, edited by K. Siegbahn (North-Holland, Amsterdam, 1966), Vol. 2, p. 997.

[10]D. C. Camp and A. L. Van Lehn, Nucl. Inst. Meth. 76, 192 (1969).

[11]The intermediate level in any cascade involving $K\alpha_2$ x rays, $L_2$, has a spin of $\frac{1}{2}$. Therefore all such cascades are isotropic.

[12]J. H. Scofield, Phys. Rev. 179, 9 (1968); Report No. UCRL-51231 (1972) (unpublished).

[13]W. Bambynek, B. Crasemann, R. W. Fink, H.-U. Freund, H. Mark, C. D. Swift, R. E. Price, and P. Venugopala Rao, Rev. Mod. Phys. 44, 716 (1972).

[14]M. R. Zalutsky and E. S. Macias, Bull. Am. Phys. Soc. 18, 635 (1973); Phys. Rev. A (to be published).

[15]M. R. Zalutsky and E. S. Macias (unpublished).

[16]J. A. Bearden, Rev. Mod. Phys. 39, 78 (1967).